J. metamorphic Geol., 2004, **22**, 579–592 doi:10.1111/j.1525-1314.2004.00534.x

Geothermobarometry of UHP and HP eclogites and schists – an evaluation of equilibria among garnet–clinopyroxene–kyanite–phengite–coesite/quartz

E. J. KROGH RAVNA[1] AND M. P. TERRY[2]
[1]*Department of Geology, University of Tromsø, N-9037 Tromsø, Norway (erling.ravna@ig.uit.no)*
[2]*Bayerisches Geoinstitut, Universität Bayreuth, D-95440 Bayreuth, Germany*

ABSTRACT Geothermometry of eclogites and other high pressure (HP)/ultrahigh-pressure (UHP) rocks has been a challenge, due to severe problems related to the reliability of the garnet–clinopyroxene Fe–Mg exchange thermometer to omphacite-bearing assemblages. Likewise, reliable geobarometers for eclogites and related HP/UHP rocks are scarce. In this paper, a set of internally consistent geothermobarometric expressions have been formulated for reactions between the UHP assemblage garnet–clinopyroxene–kyanite–phengite–coesite, and the corresponding HP assemblage garnet–clinopyroxene–kyanite–phengite–quartz. In the system KCMASH, the end members grossular (Grs) and pyrope (Prp) in garnet, diopside (Di) in clinopyroxene, muscovite (Ms) and celadonite (Cel) in phengite together with kyanite and coesite or quartz define invariant points in the coesite and quartz stability field, respectively, depending on which SiO_2 polymorph is stable. Thus, a set of net transfer reactions including these end members will uniquely define equilibrium temperatures and pressures for phengite–kyanite–SiO_2-bearing eclogites. Application to relevant eclogites from various localities worldwide show good consistency with petrographic evidence. Eclogites containing either coesite or polycrystalline quartz after coesite all plot within the coesite stability field, while typical quartz-bearing eclogites with no evidence of former coesite fall within the quartz stability field. Diamondiferous coesite–kyanite eclogite and grospydite xenoliths in kimberlites all fall into the diamond stability field. The present method also yields consistent values as compared with the garnet–clinopyroxene Fe–Mg geothermometer for these kinds of rocks, but also indicates some unsystematic scatter of the latter thermometer. The net transfer geothermobarometric method presented in this paper is suggested to be less affected by later thermal re-equilibration than common cation exchange thermometers.

Key words: geobarometry; geothermometry; high pressure; kyanite–phengite eclogite; ultrahigh pressure.

INTRODUCTION

Until fairly recently, methods for accurate pressure estimates for eclogites were not available, and commonly only minimum estimates based on the jadeite content of omphacite coexisting with quartz (in the absence of albite) could be obtained. The occasional presence of coesite or polycrystalline quartz pseudomorphs after coesite as inclusions in either garnet or omphacite (e.g. Chopin, 1984; Smith, 1984), and even microdiamonds (e.g. Okay, 1983) provided another minimum, but higher pressure limit on ultrahigh-pressure (UHP) rocks.

Waters & Martin (1993) presented a new geobarometer based on the thermodynamic data set of Holland & Powell (1990) for the fairly common eclogitic mineral assemblage garnet + clinopyroxene + phengite via the reaction

$$6\text{diopside} + 3\text{muscovite} = 2\text{grossular} + 1\text{pyrope} + 3\text{celadonite} \qquad (1)$$

This barometer has a shallow d*P*/d*T* slope with an overall estimated uncertainty of < 2 kbar, and has shown to be successful for phengite-bearing high pressure (HP) and ultrahigh-pressure (UHP) eclogites from Dabie Shan, China (Carswell *et al.*, 1997; Schmid, 2001), the Western Gneiss Complex of southern Norway (Wain, 1998; Cuthbert *et al.*, 2000; Wain *et al.*, 2001) and the Alps (Nowlan *et al.*, 2000).

Sharp *et al.* (1992) used, among other methods, the equilibrium

$$3\text{diopside} + 2\text{kyanite} = 1\text{grossular} + 1\text{pyrope} + 2\text{coesite} \qquad (2a)$$

to constrain the pressure for an ultrahigh temperature and pressure coesite–sanidine grospydite xenolith from the Roberts Victor kimberlite, South Africa. They obtained pressures of 45 ± 5 kbar at 1200 ± 100 °C for this xenolith, which are compatible with other estimates for the same sample.

Nakamura & Banno (1997) applied the equilibrium between garnet, clinopyroxene, kyanite and coesite in the CFMASH system to kyanite–coesite-bearing eclogites from Dora Maira and Su Lu. Their pressure estimates for both localities were close to or well within the stability field of coesite.

Ravna & Terry (2001) suggested that using the assemblage garnet–clinopyroxene–phengite–kyanite–SiO_2 (coesite/quartz) pressure and temperature could uniquely be defined for phengite–kyanite eclogites. This paper presents thermodynamically derived linear expressions for the *P–T–X* relationships between the end members grossular–pyrope–diopside–Al–celadonite–muscovite together with kyanite and SiO_2 (coesite or quartz) based on the database of Holland & Powell (1998). In the system KCMASH these assemblages uniquely define *P–T* conditions in UHP and HP eclogites, depending on the presence of either coesite or quartz. The clinopyroxene-absent assemblages [di, grs] have also been observed in several pelitic assemblages in UHP and HP metamorphic terranes. The geothermometric expressions presented in this paper are applied to a variety of relevant eclogites worldwide, ranging from low-temperature blueschist terranes to diamond-bearing xenoliths from kimberlites.

THE THERMODYNAMICS OF THE METHOD

In this paper, we have evaluated three linearly independent net transfer reactions among the minerals garnet–clinopyroxene–phengite–kyanite–quartz/coesite in the KCMASH system. The high-pressure assemblages are represented by the right hand side of the reactions.

(1) The kyanite–SiO_2-absent reaction [ky, coe/qtz]

$$\underset{\text{diopside}}{6\mathrm{CaMgSi_2O_6}} + \underset{\text{muscovite}}{3\mathrm{KAl_2AlSi_3O_{10}(OH)_2}} = \underset{\text{grossular}}{2\mathrm{Ca_3Al_2Si_3O_{12}}} + \underset{\text{pyrope}}{1\mathrm{Mg_3Al_2Si_3O_{12}}} + \underset{\text{celadonite}}{3\mathrm{KAlMgSi_4O_{10}(OH)_2}}, \tag{1}$$

and (2a, 2b) the phengite-absent reactions [ms, cel]

$$\underset{\text{diopside}}{3\mathrm{CaMgSi_2O_6}} + \underset{\text{kyanite}}{2\mathrm{Al_2SiO_5}} = \underset{\text{grossular}}{\mathrm{Ca_3Al_2Si_3O_{12}}} + \underset{\text{pyrope}}{\mathrm{Mg_3Al_2Si_3O_{12}}} + \underset{\text{coesite/quartz}}{2\mathrm{SiO_2}} \tag{2a, 2b}$$

with the respective equilibrium constants expressed as

$$K_1 = \frac{a_{\mathrm{pyr}}^{\mathrm{grt}}(a_{\mathrm{grs}}^{\mathrm{grt}})^2(a_{\mathrm{cel}}^{\mathrm{phe}})^3}{(a_{\mathrm{di}}^{\mathrm{cpx}})^6(a_{\mathrm{mus}}^{\mathrm{phe}})^3}$$

and

$$K_{2\mathrm{a}} = \frac{a_{\mathrm{pyr}}^{\mathrm{grt}}a_{\mathrm{grs}}^{\mathrm{grt}}(a_{\mathrm{SiO_2}}^{\mathrm{coes}})^2}{(a_{\mathrm{di}}^{\mathrm{cpx}})^3(a_{\mathrm{Al_2SiO_5}}^{\mathrm{ky}})^2} \quad K_{2\mathrm{b}} = \frac{a_{\mathrm{pyr}}^{\mathrm{grt}}a_{\mathrm{grs}}^{\mathrm{grt}}(a_{\mathrm{SiO_2}}^{\mathrm{qtz}})^2}{(a_{\mathrm{di}}^{\mathrm{cpx}})^3(a_{\mathrm{Al_2SiO_5}}^{\mathrm{ky}})^2}$$

can be simplified to the geobarometric form

$$P = A + BT + CT\ln K$$

based on the relationships between temperature, pressure and the enthalpy, entropy and molar volumes for the phases involved at approximately the centre of the chosen *P–T* windows. In these expressions $A = -\Delta H_r^{P,T}/\Delta V_r$, $B = \Delta S_r^{P,T}/\Delta V_r$, $C = -R/\Delta V_r$, $K =$ the equilibrium constant, $P =$ pressure and $T =$ temperature in K.

In addition, there are two reactions (3a, 3b), which are linear combinations of reactions (1a) and (2a, 2b), respectively, for Cpx-absent assemblages [di, grs]:

$$\underset{\text{pyrope}}{1\mathrm{Mg_3Al_2Si_3O_{12}}} + \underset{\text{muscovite}}{3\mathrm{KAl_2AlSi_3O_{10}(OH)_2}} + \underset{\text{coesite/quartz}}{4\mathrm{SiO_2}} = \underset{\text{Al-celadonite}}{3\mathrm{KAlMgSi_4O_{10}(OH)_2}} + \underset{\text{kyanite}}{4\mathrm{Al_2SiO_5}} \tag{3a, 3b}$$

$$K_{3\mathrm{a}} = \frac{(a_{\mathrm{cel}}^{\mathrm{phe}})^3(a_{\mathrm{Al_2SiO_5}}^{\mathrm{ky}})^4}{(a_{\mathrm{pyr}}^{\mathrm{grt}})(a_{\mathrm{mus}}^{\mathrm{phe}})^3(a_{\mathrm{SiO_2}}^{\mathrm{coes}})^4} \quad K_{3\mathrm{b}} = \frac{(a_{\mathrm{cel}}^{\mathrm{phe}})^3(a_{\mathrm{Al_2SiO_5}}^{\mathrm{ky}})^4}{(a_{\mathrm{pyr}}^{\mathrm{grt}})(a_{\mathrm{mus}}^{\mathrm{phe}})^3(a_{\mathrm{SiO_2}}^{\mathrm{qtz}})^4}$$

In this paper the program FRENDLY (Connolly, 1990) with the thermodynamic database of Holland & Powell (1998) were used to calculate *P–T* loci at different ln *K* values for each of the five equilibria. For reaction (1a) the *P–T* window was set to 1.0 GPa < *P* < 4.0 GPa and *T* = 500–1000 °C. For the coesite-bearing equilibria [reactions (2a) & (3a)] a *P–T* window of 2.4 GPa < *P* < 4.0 GPa and *T* = 500–1000 °C was selected, and for the equilibria involving quartz [reactions (2b) and (3b)] 3.0 GPa > *P* > 1.0 GPa and *T* = 500–1000 °C. Linear regression was performed on these data to retrieve simple relations between ln *K*, pressure and temperature for each of the reactions. Reactions (2a) and (2b) [and likewise (3a) & (3b)] are related through the coesite–quartz transition. Thus the iso-ln *K* curves for reactions (2a) and (2b) [and also for (3a) & (3b)] should intersect at the quartz-coesite transition curve. By reiteration procedures we were able to force this constraint to the final geobarometric expressions. The resulting thermobarometric expressions with regression constants for the various reactions are given in Table 1.

The present expression for reaction (1a) (Table 1) deviates from those given by Waters & Martin (1993); Waters & Martin (1996), but are similar to that given by Coggon & Holland (2002). If a kyanite–phengite-bearing eclogite equilibrated with either coesite or quartz, reactions (1a), (2a) and (3a) or (1a), (2b) and (3b) will ideally intersect at a single *P–T* point within

Table 1. Geobarometric expressions for the five reactions discussed.

Reaction	Geobarometric expression
1 [ky, qtz, coe]	P_1 (GPa) = 1.801 + 0.002781T + 0.0002425T ln K_1
2a [mu, cel, qtz]	P_{2a} (GPa) = 7.235 – 0.000659T + 0.001162T ln K_{2a}
2b [ms, cel, coe]	P_{2b} (GPa) = 11.424 – 0.001676T + 0.002157T ln K_{2b}
3a [di, grs, qtz]	P_{3a} (GPa) = −2.624 + 0.005741T + 0.0004549T ln K_{3a}
3b [di, grs, coe]	P_{3b} (GPa) = −0.899 + 0.003929T + 0.0002962T ln K_{3a}

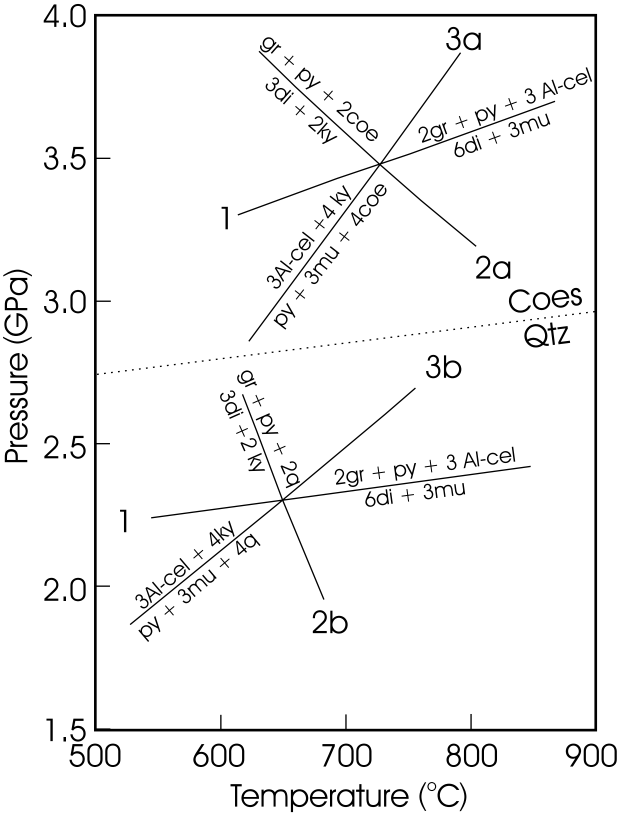

Fig. 1. Bundles of equilibrium curves for reactions (1), (2a) and (3a) for coesite- and (1), (2b) and (3b) for quartz-bearing eclogites calculated with THERMOCALC, showing the basis for the present geothermobarometric method. The curves are calculated from a theoretical set of mineral compositions. The quartz–coesite transition in this and the following figures is linearized from THERMOCALC.

the stability field of the respective SiO_2 polymorph (Fig. 1), but the linearized the expressions presented here do not produce curves that exactly intersect at a single point. The linear approach used here introduces only small divergences in calculated pressures and temperatures (< 10 °C, 0.02 GPa) as compared with those obtained by THERMOCALC. In Fig. 2 the ln$K$–P–T relationships for the reactions (1a), (2a), (2b), (3a) and (3b), based on the retrieved equations (Table 1) are shown.

The intersection of any two of these sets of reactions will uniquely define P and T for a single sample. For practical reasons, a combination of reaction (1a) (barometer) and reaction (2a) or (2b) is recommended for phengite–kyanite eclogites which have stabilized in the coesite and quartz stability fields, respectively. Reaction (1a), which has a gentle positive or negative slope in the P–T diagram, has proved to be a reliable geobarometer in phengite eclogites (Waters & Martin, 1993; Carswell *et al.*, 1997; Wain, 1998; Cuthbert *et al.*, 2000; Nowlan *et al.*, 2000; Schmid, 2001; Wain *et al.*, 2001). Using the approach from THERMOCALC (Powell & Holland, 1988) on a variety of samples, averaged standard deviations for this intersection is ± 65 °C and ± 0.32 GPa in the coesite field and ± 82 °C, ± 0.32 GPa in the quartz stability field.

Equilibrium (2a), although fairly temperature sensitive, may serve as a geobarometer in combination with the common garnet–clinopyroxene Fe–Mg geothermometer in phengite absent kyanite-bearing coesite eclogites. However, error brackets for the retrieved pressures will be large (± 0.55 GPa, ± 40 °C at *c.* 3.5 GPa/700 °C; ± 0.7 GPa and ± 70 °C at *c.* 6.0 GPa/1200 °C; THERMOCALC). Equilibria (3a) and (3b) are suggested to be useful pressure indicators for clinopyroxene-free UHP/HP pelitic schists, given that a reliable independent temperature estimate is possible. However, in the coesite stability field the slope of the iso-ln K curves for reaction (3a) is fairly steep (Fig. 2c).

An excel spreadsheet, available for download, provides the means to undertake Grt–Cpx–Ky–SiO_2 thermobarometry.

APPLICATION OF THE NEW GEOTHERMOBAROMETERS

In this paper, a combination of the activity model for the phengite solid solution proposed by Holland & Powell (1998), the clinopyroxene activity model of Holland (1990), and the garnet activity model of Ganguly *et al.* (1996) were selected (see Appendix 1). For clinopyroxene, ferric iron has been calculated assuming four cations and six oxygen. The phengite structural formula has been normalized to Σ SiAlTiCrFeMnMg = 12.00. Garnet is normalized to Σ CaMnFe^{tot} MgAlTiCr = 5.00, where $Ca + Mn + Fe^{2+} + Mg = 3.00$ and $Al + Ti + Cr + Fe^{3+} = 2.00$. Here $Fe^{3+} = 3.00 - (Al + Ti + Cr)$ and $Fe^{2+} = Fe^{tot} - Fe^{3+}$.

Maximum recordable pressure conditions for a specific eclogite should, according to reaction (4), be represented by garnet with maximum $(a^{grt}_{gr})^2 a^{grt}_{py}$, omphacite with minimum a^{cpx}_{di} (and correspondingly maximum X_{jd}) and phengite with maximum a^{phe}_{Al-cel} (maximum Si-content) (Carswell *et al.*, 2000).

The new geothermobarometric expressions have earlier been applied to UHP and HP eclogites from both the Western Gneiss Region (WGR) of Norway (Terry *et al.*, 2000; Ravna & Terry, 2001) and Greenland (Gilotti & Ravna, 2002). Below, the method is applied to a wider variety of HP and UHP rocks worldwide.

Kyanite–phengite eclogites

Western Gneiss Region, Norway

Kyanite–phengite-bearing eclogites are fairly common in the WGR of south Norway (e.g. Cuthbert *et al.*, 2000). Krabbendam & Wain (1997) defined a HP eclogite and an UHP eclogite zone separated by a mixed HP/UHP zone in the Nordfjord/Sunnmøre area of the WGR of Norway (Fig. 3). Here a series of

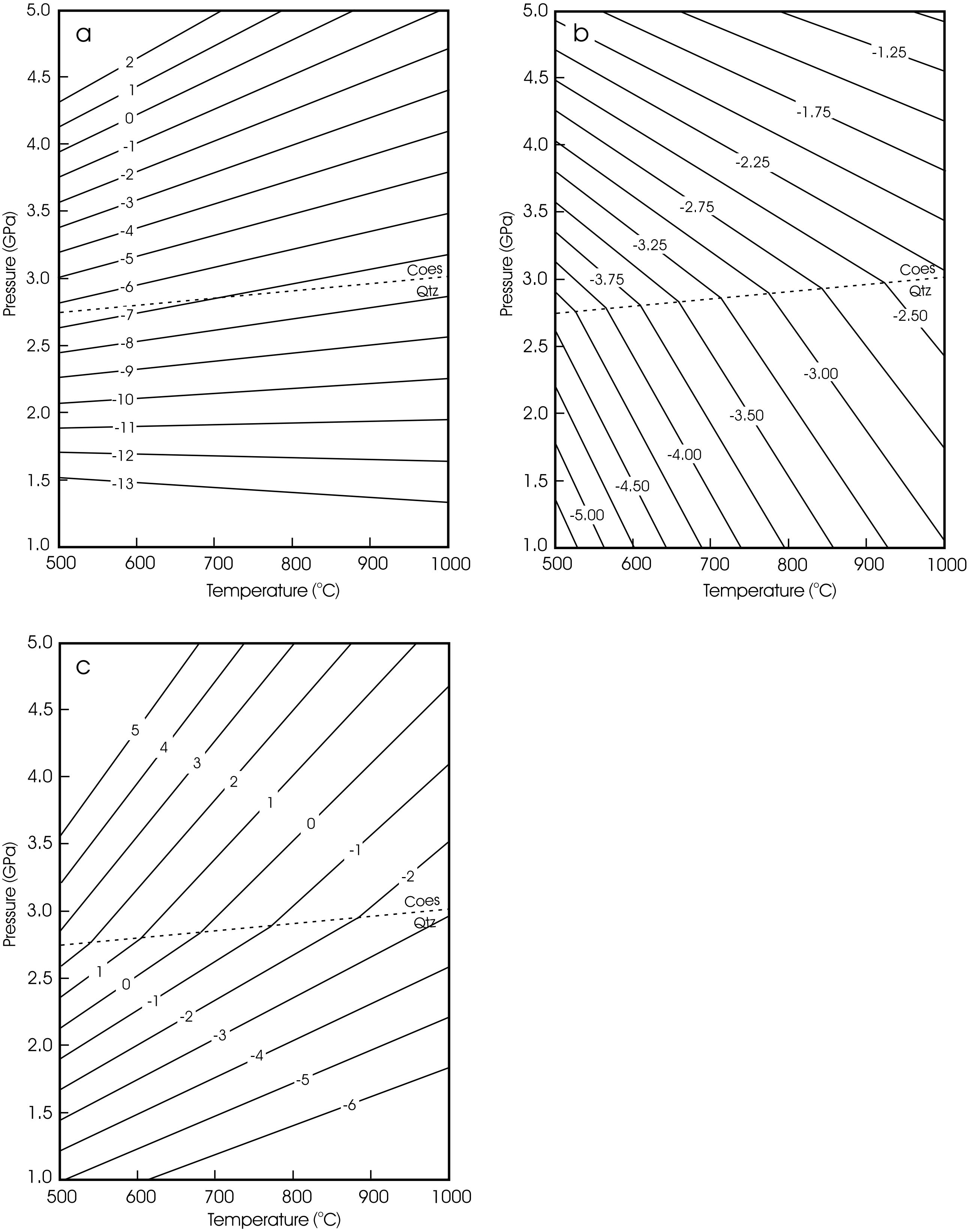

Fig. 2. Calculated iso-*lnK* curves for the five reactions described in this paper based on the linear equations described in the text. (a) Iso-*lnK* curves for reaction 1; (b) Iso-*lnK* curves for reactions (2a) and (2b); (c) Iso-*lnK* curves for reactions (3a) and (3b).

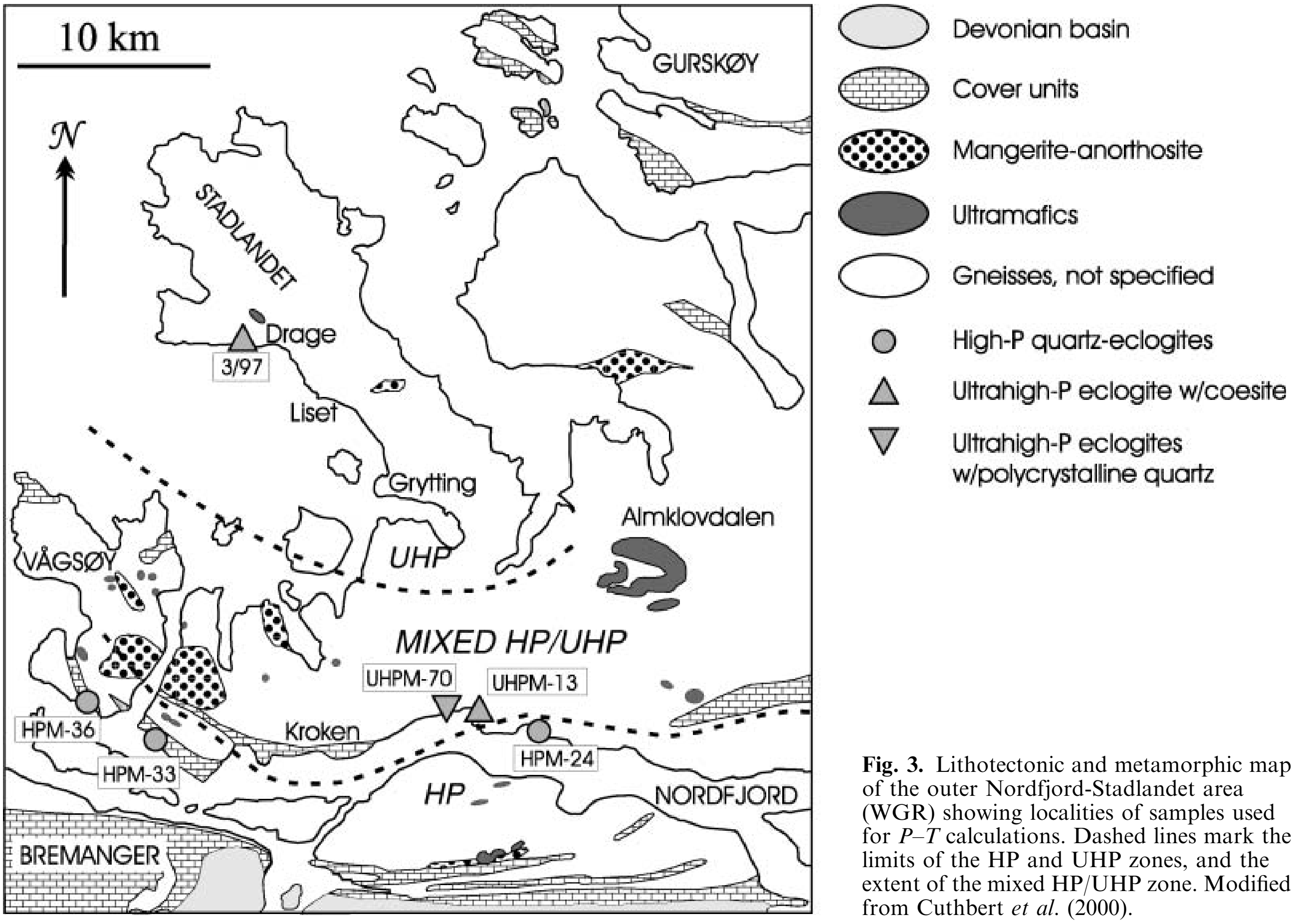

Fig. 3. Lithotectonic and metamorphic map of the outer Nordfjord-Stadlandet area (WGR) showing localities of samples used for *P–T* calculations. Dashed lines mark the limits of the HP and UHP zones, and the extent of the mixed HP/UHP zone. Modified from Cuthbert *et al.* (2000).

garnet–clinoyproxene–phengite–kyanite–SiO_2 assemblages from the WGR of Norway have been chosen from the dataset of Cuthbert *et al.* (2000). Mineral compositions of suggested maximum pressure conditions (see above) are presented in Tables 2–4. The samples were analyzed with a JEOL 840 SEM with an EDAX EDS analyzer, using the EDAX SEM-Quant standardless method with optimized SEC factors based on analyses of various mineral standards. Data reduction was done by the ZAF method. All totals are normalized to 100%. Operating conditions were 20 kV accelerating voltage and a beam current of 3×10^{-9} A.

Three of the selected WGR samples (3/97, UHPM-13, UHPM-70) from north of and within the mixed HP/UHP zone (Fig. 3) either contain coesite and/or polycrystalline quartz after coesite. Garnet from these eclogites commonly show no zoning, except from the outer rim where the Mg# and X_{Ca} drop. Phengite commonly has high Si cores and lower Si rims, with a fairly regular increase in Fe/Mg with decreasing Si. Omphacite shows only minor zoning. These features are ascribed to diffusional adjustments during uplift. Three other samples (HPM-24, HPM-36 & HPM-33) from just south of the mixed zone (Fig. 3) have garnet with strong prograde growth zoning, and show no evidence for the former presence of coesite. *P–T* conditions are calculated for the supposed maximum pressure compositions, as described above. The results of these calculations are presented in Fig. 4a and Table 5. The samples containing relict coesite and/or polycrystalline quartz all fall well within the coesite stability field, while those showing no evidence for former coesite all fall into the quartz stability field. Also note that temperatures calculated with the Grt–Cpx Fe–Mg geothermometer (Ravna, 2000) for all these samples are within error of those of the present method.

Dabie Shan, China

Two quartz-bearing (CD107 and DB53 from Huangzhen) and one coesite-bearing sample (CD48 from Bixilian) of phengite–kyanite eclogite from Dabie Shan (Carswell *et al.*, 1997) have also been recalculated here using the combination of the garnet–clinopyroxene–phengite barometer and the garnet–clinopyroxene–kyanite–coesite thermometer. The coesite-bearing eclogite plots well into the coesite stability field at 3.70 GPa and 794 °C, not far from the graphite–diamond transition, while the two quartz-bearing samples, both with well-pronounced prograde growth zoned garnet, plot well within the quartz stability field (CD107: 2.47 GPa/545 °C; DB53: 2.52 GPa/502 °C),

Table 2. Analyses of garnet from UHP and HP eclogites from the WGR used in calculations of P–T conditions presented in Fig. 4a, c.

Sample	3/97	UHPM-70	UHPM-13	HPM-36	HPM-24	HPM-33	194	194
Locality	Drage (Max P)	Totland (Max P)	Maurstad (Max P)	Halnes (Max P)	Levdal (Max P)	Skavøy-pollen (Max P)	Kvineset (Max P)	Kvineset (Inclusion)
SiO_2	39.85	38.87	39.40	39.57	38.92	38.25	37.93	37.07
TiO_2	0.16	0.27	0.17	0.00	0.13	0.28	NA	NA
Al_2O_3	22.18	21.83	21.63	21.82	21.26	21.68	21.78	21.57
FeO	16.19	21.05	20.93	21.35	23.23	23.55	27.35	29.46
MnO	0.52	0.59	0.54	0.19	0.72	0.47	0.77	0.24
MgO	11.41	6.89	8.40	7. 80	7.59	6.97	5.40	3.90
CaO	9.70	10.50	8.93	9.28	8.14	8.81	6.47	7.42
Total	100.01	100.00	100.00	100.00	99.99	100.00	99.70	99.86
Recalculated to $\Sigma\ Y = 2.00$ and $\Sigma\ X = 3.00$								
Al	1.93	1.96	1.94	1.97	1.92	1.95	2.00	1.99
Ti	0.01	0.02	0.01	0.00	0.01	0.02	0.00	0.00
Fe^{3+}	0.06	0.02	0.05	0.03	0.07	0.04	0.00	0.01
Sum Y	2.00	2.00	2.00	2.00	2.00	2.00	2.00	2.00
Fe^{2+}	0.94	1.32	1.28	1.34	1.42	1.46	1.78	1.91
Mn	0.03	0.04	0.03	0.01	0.05	0.03	0.05	0.02
Mg	1.26	0.78	0.95	0.89	0.87	0.79	0.63	0.45
Ca	0.77	0.86	0.73	0.76	0.67	0.72	0.54	0.62
Sum X	3.00	3.00	3.00	3.00	3.00	3.00	3.00	3.00

Table 3. Analyses of omphacite from UHP and HP eclogites from the WGR used in calculations of P–T conditions presented in Fig. 4a, c.

Sample	3/97	UHPM-70	UHPM-13	HPM-36	HPM-24	HPM-33	194	194
Locality	Drage (Max Jd)	Totland (Max Jd)	Maurstad (Max Jd)	Halnes (Max Jd)	Levdal (Max Jd)	Skavøy-pollen (Max Jd)	Kvineset (Max Jd)	Kvineset (Inclusion)
SiO_2	55.45	56.33	56.25	56.60	56.26	56.33	55.81	54.78
TiO_2	0.13	0.11	0.17	0.21	0.16	0.12	NA	NA
Al_2O_3	9.62	12.73	11.04	11.46	11.00	12.56	11.22	9.62
FeO	2.53	3.45	3.69	3.43	3.70	4.44	7.44	8.77
MnO	0.06	0.15	0.13	0.12	0.16	0.13	0.05	0.06
MgO	10.64	7.82	8.53	8.45	8.56	7.05	6.48	6.53
CaO	16.22	11.69	13.06	12.56	13.13	11.25	10.03	10.72
Na_2O	5.35	7.72	7.11	7.20	7.04	8.13	8.58	8.13
Total	100.00	100.00	100.00	100.01	100.00	100.00	99.61	98.61
4 cations; 6 oxygen								
Si	1.97	1.98	1.99	2.00	1.99	1.99	1.99	1.98
Al(IV)	0.03	0.02	0.01	0.00	0.01	0.01	0.01	0.02
Al(VI)	0.37	0.51	0.45	0.48	0.45	0.51	0.46	0.39
Ti	0.00	0.00	0.00	0.01	0.00	0.00	NA	NA
Fe^{3+}	0.02	0.03	0.04	0.01	0.03	0.05	0.15	0.19
Fe^{2+}	0.05	0.08	0.07	0.10	0.08	0.08	0.07	0.07
Mn	0.00	0.00	0.00	0.00	0.00	0.00	0.00	0.00
Mg	0.56	0.41	0.45	0.44	0.45	0.37	0.34	0.35
Ca	0.62	0.44	0.50	0.48	0.5	0.43	0.38	0.42
Na	0.37	0.53	0.49	0.49	0.48	0.56	0.59	0.57
Cations	4.00	4.00	4.00	4.00	4.00	4.00	4.00	4.00

approaching the lawsonite–eclogite field of Okamoto & Maruyama (1999). In both cases our method gives substantial lower temperature and higher pressure than those calculated by Carswell *et al.* (1997) for the same samples, using the garnet–clinopyroxene thermometer of Powell (1985) combined with the Waters & Martin (1993) garnet–clinopyroxene–phengite barometer (Fig. 4b, Table 5). We have also recalculated P–T conditions for the other kyanite-free phengite eclogites described by Carswell *et al.* (1997), and the results are given in Table 5 together with the corresponding results from Carswell *et al.* (1997), and also plotted in Figs 4b and 5b. The pressure differences between our calculations and those of Carswell *et al.* (1997) stems both from the choice of garnet activity model and the different geobarometric expressions obtained for the garnet–clinopyroxene–phengite barometer.

Other eclogites

Kyanite-free low-T phengite–eclogites related to blueschists

Low-T phengite eclogites lack kyanite – thus the use of the internally consistent thermobarometers presented here cannot be used in full. Instead, a combination of reaction (1a) and the garnet–clinopyroxene Fe–Mg thermometer (Ravna, 2000) may be used. Figure 4c shows the result of calculations on two samples of glaucophane-bearing phengite–eclogite, one from the Franciscan at Jenner, CA, USA (Krogh *et al.*, 1994), and one from Kvineset, WGR, Norway (Krogh, 1980). Interestingly, both samples fall close to the blueschist–eclogite facies transition of Okamoto & Maruyama (1999), the Franciscan sample within the lawsonite

Table 4. Analyses of phengite from UHP and HP eclogites from the WGR used in calculations of *P–T* conditions presented in Fig. 4a, c.

Sample Locality	3/97 Drage (Max Si)	UHPM-70 Totland (Max Si)	UHPM-13 Maurstad (Max Si)	HPM-36 Halnes (Max Si)	HPM-24 Levdal (Max Si)	HPM-33 Skavøy-pollen (Max Si)	194 Kvineset (Max Si)	194 Kvineset (Inclusion)
SiO_2	55.45	53.88	55.80	52.37	53.02	52.26	50.20	49.70
TiO_2	0.63	0.57	0.44	0.78	0.83	0.83	0.40	0.40
Al_2O_3	26.33	27.36	26.39	29.80	29.67	29.59	26.97	27.17
FeO	1.67	1.89	1.59	2.05	1.94	2.25	3.13	3.03
MnO	0.00	0.00	0.15	0.00	0.00	0.00	0.00	0.00
MgO	4.60	4.85	4.70	3.87	3.14	4.00	3.43	3.54
CaO	0.00	0.17	0.13	0.00	0.19	0.00	0.00	0.00
Na_2O	0.76	1.17	1.08	1.30	1.47	1.33	0.71	0.71
K_2O	10.56	10.11	9.70	9.84	9.74	9.73	10.71	10.71
Total	100.01	100.00	99.99	100.01	100.00	99.99	95.55	95.26
Cations – A = 12.00								
Si	6.99	6.78	7.00	6.58	6.70	6.56	6.69	6.64
Aliv	1.01	1.22	1.00	1.42	1.30	1.44	1.31	1.36
Alvi	2.90	2.84	2.90	2.99	3.12	2.94	2.93	2.92
Ti	0.06	0.05	0.04	0.07	0.08	0.08	0.04	0.04
Fe^{tot}	0.18	0.20	0.17	0.22	0.20	0.24	0.35	0.34
Mn	0.00	0.00	0.02	0.00	0.00	0.00	0.00	0.00
Mg	0.86	0.91	0.88	0.72	0.59	0.75	0.68	0.70
Ca	0.00	0.02	0.02	0.00	0.03	0.00	0.00	0.00
Na	0.18	0.29	0.26	0.32	0.36	0.32	0.18	0.18
K	1.70	1.62	1.55	1.58	1.57	1.56	1.82	1.83
Cations	13.88	13.93	13.83	13.89	13.96	13.88	14.00	14.01

eclogite field at higher pressure (2.21 GPa) and slightly lower temperature (*c.* 434 °C) than the WGR sample, which shows increasing pressure with increasing temperature based on inclusion (1.85 GPa, 430 °C) and rim compositions (2.04 GPa, 509 °C), respectively, indicating continuous prograde growth. Krogh *et al.* (1984) gave *minimum* pressures of 1.2–1.3 GPa at 450–500 °C for the Jenner locality. Cuthbert *et al.* (2000) reported maximum pressures (1.62–1.82 GPa) for Kvineset using the Waters & Martin (1993) barometer with garnet activities from Berman (1990).

Eclogites and omphacite-free garnetiferous kyanite–phengite gneisses and schists from the Adula-Cima Lunga unit, Central Alps

Heinrich (1986) described five eclogites from a north-south cross-section through the Adula-Cima Lunga unit. Going southwards from Vals, Heinrich (1986) reported the following general trend of increasing *P-T*: Vals: 1.0–1.3 GPa, 450–550 °C; Confin: 1.2–2.2 GPa, 450–550 °C; Trescolmen: 1.5–2.2 GPa, 550–650 °C; Gagnone: 1.5–2.5 GPa, 600–700 °C; Arami: 1.8–3.5 GPa, 750–900 °C (Table 5). For the low-temperature Vals eclogite pressure was estimated from the assumed equilibrium assemblage omphacite–albite–quartz. For the other localities, the lower pressure limits were put at the stability of Jd_{50} + quartz. Upper pressure limits for Confin and Trescolmen were determined from the upper stability of paragonite, while the Al-content of orthopyroxene in garnet lherzolites was used for the upper pressure limit of the Gagnone and Alpe Arami eclogites. Meyre *et al.* (1999) reported peak pressure conditions of *c.* 2.5 GPa (maximum pressure stability of quartz) at 600–700 °C for Trescolmen, based on calculated equilibrium phase diagrams of sodic whiteschist (Z6-50-12). Nimis & Trommsdorff (2001a)) presented new thermobarometric data of on garnet lherzolites from Cima di Gagnone (3.0 ± 0.4 GPa, 740 ± 38 °C) and Alpe Arami (3.2 ± 0.3 GPa, 844 ± 23 °C). Paquin & Altherr (2001a) got much higher values (5.9 ± 0.3 GPa, 1180 ± 40 °C) for the Alpe Arami peridotite body based on homogeneous cores of porphyroclasts. They claimed that the former *P–T* results for this body were erroneously based on non-equilibrium assemblages. In a discussion letter Nimis & Trommsdorff (2001b)) said that their result represented a later low-*T* stage representative of the Alpine subduction metamorphism. In a reply Paquin & Altherr (2001b) upheld their arguments, and concluded that the eclogites and peridotites were tectonically amalgamated after equilibration of the eclogites at 750–800 °C. Dobrzinetskaya *et al.* (2002) described exsolved SiO_2 in omphacite from the Alpe Arami eclogite, and calculated the invariant point for reactions among the end-members Alm–Prp–Grs–Di–Hd–CaTs at 7.04 GPa, 1118 °C.

In this paper we have recalculated pressures and temperatures for some of the samples where mineral chemical data are available in the literature. Eclogite samples from Alpe Arami containing garnet–omphacite–kyanite–quartz from Ernst (1977), sample (F-53) and Heinrich (1986), sample (Mg9-5-2c) give 3.20 GPa, 764 °C and 3.49 GPa, 676 °C, respectively, by a combination of the Grt–Cpx–Ky–SiO_2 and Grt–Cpx Fe–Mg equilibria. Heinrich's (1986) samples from Vals (Ad42-9-14) and Confin (Ad48-9-5) give 1.88 GPa, 484 °C and 2.26 GPa, 512 °C, respectively, by combining the Grt–Cpx–Phe barometer and the Grt–Cpx Fe–Mg thermometer. Recalculated *P–T* values for Heinrich's samples from Trescolmen (Ad25-9-3) and Gagnone (CH271) are 2.91 GPa, 650 °C and 3.11 GPa, 624 °C, respectively, using a combination of the Grt–Cpx–Ky–SiO$_2$ and Grt–Cpx–Phe equilibria. Another sample (Z6-50-13) from Trescolmen containing Grt–Cpx–Phe–Ky–Qtz (Zack *et al.*, 2001, 2002) gives 2.78 GPa, 667 °C.

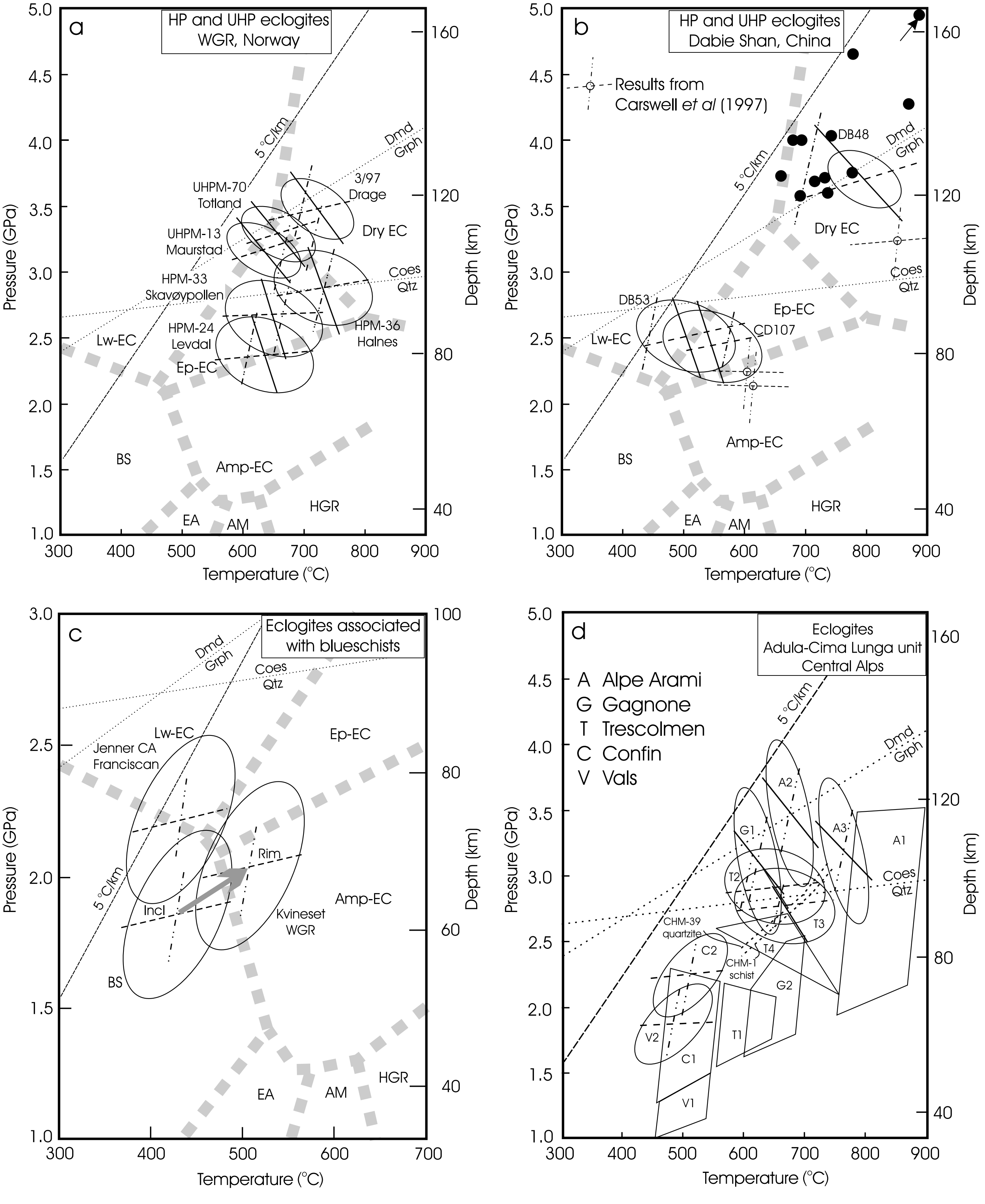

Reactions (3a) and (3b) may be used as pressure indicators in clinopyroxene-free garnetiferous kyanite–phengite schists, if an independent temperature estimate can be achieved. We have applied this method on coexisting garnet and phengite from garnet-phengite-kyanite schist and quartzite (CHM-1 & CHM-39; Meyre *et al.*, 1999) from Trescolmen. The calculated garnet–phengite–kyanite–SiO_2 curves for the samples CHM-1 and CHM-39 pass close to the intersection between the Grt–Cpx–Ky–Qtz and Grt–Cpx–Phe curves for sample Z6-50-13 (Fig. 4d), just below the quartz-coesite transition, showing the isofacial character of eclogite and schist in the area.

Phengite-free xenoliths of coesite–kyanite eclogites and grospydites from kimberlites

At increasing pressure the equilibrium curve for reaction (2a) gradually becomes less steep, and may serve as a barometer (e.g. Sharp *et al.*, 1992). However, at these extreme conditions large errors are introduced to the geobarometric results (Fig. 5a). The combination of reaction (1) and the Grt–Cpx Fe–Mg thermometer (Ravna, 2000) has been applied to five samples from the Roberts Victor Mine (Group I), South Africa (Sharp *et al.*, 1992; Schulze *et al.*, 2000), three samples from Lace, South Africa and four samples from Zagadochnaya, Yakutia (Schulze & Helmstaedt, 1988). Figure 5a shows that the Roberts Victor and Lace samples all fall within the diamond field, but at higher pressures than the average 'Lesotho geotherm' defined by Carswell & Gibb (1987). The non-diamondiferous grospydites from Zagadochnaya (Schulze & Helmstaedt, 1988) all fall in the graphite + coesite field, on the high-*T* side of the 'Lesotho geotherm'.

DISCUSSION

Thermometry of eclogites is mainly performed using one or more of the many versions of the Grt-Cpx Fe-Mg thermometer (e.g. Ellis & Green, 1979; Powell, 1985; Krogh, 1988; Pattison & Newton, 1989; Ai, 1994; Ravna, 2000). The main problem concerning this method is the uncertainty related to the oxidation state of iron. The commonly accepted method for estimation of Fe^{3+}/Fe^{tot} by charge balance has lately been disputed (e.g. Canil & O'Neill, 1996; Carswell & Zhang, 1999; Sobolev *et al.*, 1999; Schmid *et al.*, 2003; Ravna & Paquin, 2004). Ravna & Paquin (2004) have shown that for a single sample, 40 individual spot analyses of homogeneous omphacite combined with a single-spot analysis of garnet gave a total spread in Grt–Cpx temperatures of 646–914 °C at 4.0 GPa, with a mean of 867 ± 58. The large spread is ascribed to variations introduced by the widely accepted calculation of Fe^{2+}/Fe^{3+} by assumption of stoichiometry (four cations and six oxygen) of clinopyroxene as there is a clear negative correlation between the calculated Fe^{3+}/Fe^{tot} and temperature. Schmid (2001) analyzed the Fe^{2+} content of clinopyroxene in the same sample by standard titration methods, and calculated a Fe^{3+}/Fe^{tot} ratio of 0.35. Using this value, calculated temperatures become 758 ± 12 °C. This shows that the reliability of the Grt–Cpx Fe–Mg thermometer is highly fragile. Carswell & Zhang (1999) suggested that even with high quality EMP analyses, error brackets of ±100 °C should be attached to individual garnet–clinopyroxene Fe^{2+}-Mg estimates simply because of uncertainties regarding the proportions of Fe^{3+} and Fe^{2+} in omphacite. In addition, later thermal overprint may cause partial to total redistribution of Fe^{2+} and Mg between garnet and clinopyroxene, and thus obscure the result even more. The reliability of the widely used Grt–Cpx Fe–Mg thermometer is thus overestimated, and the commonly cited uncertainty of ±30 °C is most probably far too optimistic. According to the result given by Ravna & Paquin (2004) it should rather be about ±60 °C. The present method involving garnet–clinopyroxene–kyanite–SiO_2 should be regarded as an alternative and more robust method for temperature estimation, even with error brackets of ±65 °C in the coesite and ±85 °C in the quartz field (1σ; THERMOCALC).

The Grt–Cpx–Phe barometer presented here gives invariably higher pressures (Table 5) than the corresponding method of Waters & Martin (1993). This stems both from the different barometric expressions and the preferred garnet activity model, as the latter authors use the model of Newton & Haselton (1981). However, if the garnet activity models of either Berman (1990) or Ganguly *et al.* (1996) is used with

Fig. 4. (a) Calculated maximum *P* conditions for three kyanite–phengite bearing UHP and three HP eclogites from the WGR (see locations in Fig. 3). The error ellipses are based on values from THERMOCALC. Metamorphic facies grid is from Okamoto & Maruyama (1999). The graphite–diamond transition curve in this and the following figures is linearized from THERMOCALC. (b) Calculated *P–T* conditions for two HP and one UHP phengite–kyanite eclogite from Dabie Shan, China (Carswell *et al.*, 1997). The estimates of Carswell *et al.* (1997) are also shown. Dots show the results for kyanite-free UHP samples (Carswell *et al.*, 1997) resulting from a combination of the Grt–Cpx–Phe barometer (this paper) and the Grt–Cpx thermometer (Ravna, 2000). (c) Calculated *P–T* conditions for low-*T* (blueschist type) kyanite-free phengite eclogites from the SE part of the WGR (Krogh, 1980) and the Franciscan Formation (Krogh *et al.*, 1994), using a combination of reaction (1a) and the Grt–Cpx thermometer (Ravna, 2000). (d) *P–T* estimates for eclogites and associated gneisses from Adula Nappe, western Alps. Estimates from Heinrich (1986) are shown as V1, C1, T1, G1 and A1. Corresponding estimates on the same samples by the present method are V2, C2, T2, G2 and A2. A3 is sample F-53 from Ernst (1977), T3 is sample Z6-50-13 from Trescolmen (Zack *et al.*, 2001, 2002) calculated by the present method, and T4 is the calculated peak pressure stability for whiteschist Z6-50-12 from Trescolmen (Meyre *et al.*, 1999). The garnet–phengite–kyanite–SiO_2 curves for the garnet–white mica–kyanite schist CHM-1 and quartzite CHM-39 from Trescolmen (Meyre *et al.*, 1999) is also shown. Curve symbols as given in (Fig. 4.).

Table 5. Estimated pressures (in GPa) and temperatures (in °C) for eclogites discussed in the text. For Lance no previous data are available.

Sample	P_{RT}	T_{RT}	Method	P_o	T_o	Method	Reference
WGR							
3/97	3.46	727	1 & 2	3.18	768	4 & 5	Cuthbert *et al.*, 2000
UHPM-70	3.29	658	1 & 2	3.10	769	4 & 5	Cuthbert *et al.*, 2000
UHPM-13	3.21	637	1 & 2	3.04	706	4 & 5	Cuthbert *et al.*, 2000
HPM-36	2.88	729	1 & 3	2.52	738	4 & 5	Cuthbert *et al.*, 2000
HPM-24	2.37	639	1 & 3	2.41	655	4 & 5	Cuthbert *et al.*, 2000
HPM-33	2.69	649	1 & 3	2.29	575	4 & 5	Cuthbert *et al.*, 2000
194 max-P	2.04	509	1 & 4	1.80	517	4 & 5	Cuthbert *et al.*, 2000
194 incl	1.85	430	1 & 4				
Adula-Cima Lunga							
Vals							
Ad42-9-14	1.92	485	1 & 4	1.0–1.3	450–550	see text	Heinrich, 1986
Confin							
Ad48-9-5	2.30	514	1 & 4	1.2–2.2	450–550	see text	Heinrich, 1986
Trescolmen							
Ad25-9-3	2.94	655	1 & 2	1.5–2.2	550–650	see text	Heinrich, 1986
Z6-50-13	2.78	667	1 & 3				
Gagnone							
CH271	3.19	628	2 & 4	1.5–2.5	600–700	see text	Heinrich, 1986
Alpe Arami							
Mg9-5-2c	3.56	679	2 & 4	1.8–3.5	750–900	see text	Heinrich, 1986
Dabie Shan							
Dongfeng							
CD10	3.77	775	1 & 4	2.98	740	4 & 5	Carswell *et al.*, 1997
Shima							
CD16	3.60	732	1 & 4	3.69	841	4 & 5	Carswell *et al.*, 1997
CD18	5.30	945	1 & 4	3.98	851	4 & 5	Carswell *et al.*, 1997
CD20	4.25	886	1 & 4	3.51	882	4 & 5	Carswell *et al.*, 1997
CD99	4.01	682	1 & 4	3.40	676	4 & 5	Carswell *et al.*, 1997
Shuanghe							
CD33	3.69	708	1 & 4	3.08	687	4 & 5	Carswell *et al.*, 1997
CD34	3.73	724	1 & 4	3.33	744	4 & 5	Carswell *et al.*, 1997
CD35	4.03	742	1 & 4	3.42	707	4 & 5	Carswell *et al.*, 1997
Guanjiling							
CD40	3.59	696	1 & 4	3.41	863	4 & 5	Carswell *et al.*, 1997
CD41	4.01	697	1 & 4	3.83	867	4 & 5	Carswell *et al.*, 1997
Bixilian							
CD47	4.69*	787*	1 & 4	3.73	833	4 & 5	Carswell *et al.*, 1997
CD48	3.70	794	1 & 2	3.23	879	4 & 5	Carswell *et al.*, 1997
Huangzhen							
CD107	2.47	545	1 & 3	2.14	614	4 & 5	Carswell *et al.*, 1997
DB53	2.52	502	1 & 3	2.24	605	4 & 5	Carswell *et al.*, 1997
Rongcheng							
	3.74	668	2 & 4	3.4	790	6	Nakamura & Banno, 1997
Roberts Victor							
SRV-1	5.86	1166	2 & 4	4.5 ± 0.5	1200 ± 100	7	Sharp *et al.*, 1992
SRV-1	5.82	1178	2 & 4				
13-64-100	6.28	1210	2 & 4				
13-64-104	5.96	1169	2 & 4				
13.64-107	5.34	1159	2 & 4				
13-64-109	5.95	1153	2 & 4				
Lace							
1365-2	5.09	1095	2 & 4				
1365-8	4.72	1004	2 & 4				
1365-16	4.73	1014	2 & 4				
Zagadochnaya							
Z-00	3.44	1005	2 & 4				
Z-39	3.15	989	2 & 4				
Z-46	3.24	1056	2 & 4				
Z-55	3.83	1018	2 & 4				
Various samples				3.2–4.0	650–800	8	Dencker *et al.*, 2003

Methods: 1, Grt–Cpx–Phe (this paper); 2, Grt–Cpx–Ky–Coes; 3, Grt–Cpx–Ky–Qtz; 4, Grt–Cpx Fe–Mg; 5, Grt–Cpx–Phe (Waters & Martin, 1993); 6, Grt–Cpx–Ky–Coes (Nakamura & Banno, 1997); 7, various methods; 8, single-Cpx geothermobarometry (Nimis & Taylor 2000).

P_{RT} and T_{RT} are pressure and temperature estimates from this paper.

P_O and T_O are pressure and temperature estimates from the original papers.

the Waters & Martin (1993) method, pressure becomes about 0.2 GPa higher (e.g. Cuthbert *et al.*, 2000).

The present values for eclogites (Table 5) from the WGR of Norway, Adula-Cima Lunga unit of the Alps and Dabie Shan apparently define a *P–T* array of 6–7 °C km^{-1} up to *c.* 4.0 GPa, 800 °C (Fig. 5b). An extrapolation of this trend to higher *P* and *T* values passes straight through the maximum conditions of *c.* 5.9 GPa, 1180 °C for the Alpe Arami peridotite body (Paquin & Altherr, 2001a), and the *P–T* fields calculated here for the Lace and Roberts Victor xenoliths. The present trend also passes through the lower part of the *P–T* field of representative Dabie-Sulu eclogites and garnet peridotites suggested by Liou *et al.* (2002).

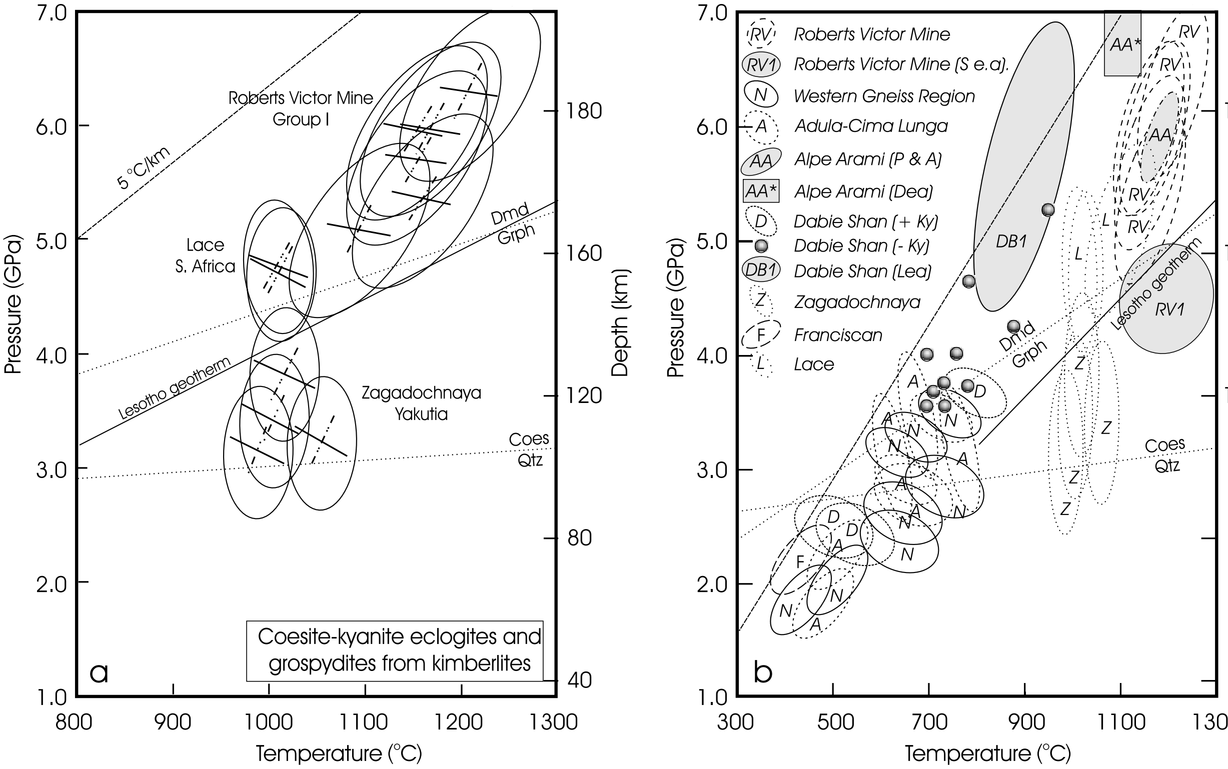

Fig. 5. (a) *P–T* estimates for coesite–kyanite eclogites and grospydites from kimberlites. The combination of reaction (2a) and the garnet–clinopyroxene Fe/Mg thermometer (Ravna, 2000) has been applied to five Group I samples from the Roberts Victor Mine (Sharp *et al.*, 1992; Schulze *et al.*, 2000), three samples from Lace, South Africa, and four samples from Zagadochnaya, Yakutia (Schulze & Helmstaedt, 1988). The Lesotho geotherm is taken from Carswell & Gibb (1987). Curve symbols as given in (Fig. 4). (b) Summary of the present calculations on HP-UHP samples from various localities and settings. As reference the maximum *P–T* estimates for the Alpe Arami peridotite (AA) from Paquin & Altherr (2001a)) and for the adjacent eclogite (AA*) from Dobrzinetskaya *et al.* (2002) is shown, as well as the estimates for Roberts Victor (RV1) from Sharp *et al.* (1992) and the array of *P–T* estimates for Dabie and Sulu (DB1) given by Liou *et al.* (2002).

The distinction of the UHP and HP eclogites from the WGR shown here (Fig. 4a) is apparently very clear. However, Cuthbert *et al.* (2000) showed that there seems to be a more or less continuum of *P–T* conditions across the entire WGR, from lower to higher *P–T* going from south to north. Of more interest is the large pressure difference of 0.8 GPa recorded over a distance of 2–2.5 km between the UHP eclogite at Maurstad (UHPM-13: 3.17 GPa and 645 °C) and the HP eclogite at Levdal (HPM-24: 2.37 GPa and 639 °C). At least two hypotheses can be promoted for such a situation: (1) There is a major tectonic break between these two localities; and (2) The eclogites at both localities were subjected to the same UHP conditions, but the eclogite at Levdal for some reason froze at the lower pressure conditions and failed to respond to the maximum pressure conditions. To solve this problem, detailed mapping and sampling in this area has to be performed.

Maximum pressure conditions for the Alpe Arami eclogite appears to be around 3.5 GPa at 650–750 °C based on the Grt–Cpx–Ky–Coes equilibrium combined with the Grt–Cpx Fe–Mg thermometer, which is far below the maximum conditions (*c.* 7.0 GPa, 1100 °C) obtained by Dobrzinetskaya *et al.* (2002). Their pressure estimate is, however, very sensitive to the accuracy of determination of the Ca-Tschermak's component in the omphacite (Dobrzinetskaya *et al.*, 2002). The present result is also apparently different from their uplift stage IIb at 3.7 GPa, 950 °C. However, Dobrzinetskaya *et al.* (2002) stated that their thermodynamically calculated temperature estimates are about (or at least) 70 °C higher at a given pressure than those obtained by the garnet–clinopyroxene Fe–Mg thermometer. Taken this into consideration, and combining it with the large uncertainties of the latter method, their conditions for stage IIb appear to be equal to our maximum conditions for the Alpe Arami eclogite. If the reported assemblage garnet–omphacite–kyanite–SiO_2 in the samples analyzed by Ernst (1977) and Heinrich (1986) really represent equilibrium at maximum pressure conditions, maximum pressures could not have been greatly in excess of 3.5 GPa according to the present calculations (Fig. 4d) due to the negative slope of the equilibrium curve for this assemblage. This is thus in conflict with the very high pressures given by Dobrzinetskaya *et al.* (2002).

As the HP and UHP eclogites from various collisional belts as the Scandinavian Caledonides, the Alps and Dabie-Sulu certainly are products of processes involving deep subduction of crustal material, there has been some dispute of whether mantle eclogite xenoliths represent subducted oceanic crust or residues of partial melting. Schulze *et al.* (2000) concluded that their oxygen isotope data on the Roberts Victor eclogites, together with the presence of free silica, are consistent with a model in which the protoliths were oceanic basalts and intrusive rocks that were subducted to and metamorphosed at UHP conditions. In Fig. 5b it appears that the South African xenolithic eclogites grossly lie along the extension of the *P–T* array defined by crustal eclogites, which supports this conclusion. The grospydite xenoliths from Zagadochnaya apparently were equilibrated along a different and warmer *P*/*T* gradient according to the present results (Fig. 5b). Dencker *et al.* (2003) presented *P–T* estimates for Zagadochnaya diopside that they assumed were derived from a garnet peridotite, using the single-Cpx thermobarometers of Nimis & Taylor (2000). The majority of their samples cluster within 3.2–4.0 GPa, 650–800 °C, close to the graphite–diamond boundary, along a geothermal gradient similar to that of the Lance and Roberts Victor xenoliths. The discrepancy between the present results and those of Dencker *et al.* (2003) is not understood.

CONCLUSIONS

The present paper demonstrates the potential of the fairly common eclogite assemblage garnet–clinopyroxene–phengite–kyanite–coesite/quartz as a unique geothermobarometer. The present set of geothermobarometric expressions has uncertainties in estimated *P* and *T* which are comparable to pre-existing ones. In addition they offer some advantages:

(1) The thermobarometric expressions are based on net-transfer reactions between common HP/UHP minerals. Net-transfer reactions are known to be more robust against resetting during uplift/heating and cooling than the commonly used cation exchange thermometers.

(2) The expressions are based on Mg end members, which imply that uncertainties involving Fe^{2+}/Fe^{3+} ratios are virtually absent, or at least minimal. The end members are major components of common minerals.

(3) The expressions are internally consistent. Although the absolute values of temperature and pressure may be somewhat inaccurate, the present method with a combination of the Grt–Cpx–Phe and the Grt–Cpx–Ky–SiO_2 equilibria will give a consistent relative pattern of *P–T* values, and may also be useful in the calculation of specific *P–T* paths.

(4) For the samples used here for application, calculated pressures appear to be consistent with petrogenetic grids, including the presence of either quartz, coesite, graphite or diamond.

ACKNOWLEDGEMENTS

Valuable comments from A. Patiño-Douce, D.A. Carswell, P. Robinson and the referees D. Waters and G. Markl greatly improved this paper. A special thank to E. Ellingsen who carefully prepared the WGR samples used in this paper.

SUPPLEMENTARY MATERIAL

An excel spreadsheet for Grt–Cpx–Phe–Ky–SiO_2 thermobarometry is available for download from http://www.blackwellpublishing.com/products/journals/suppmat/JMG/JMG534/JMG534sm.htm. The file GCPKS.doc is an instruction guide to running GCPKS.xls.

REFERENCES

Ai, Y., 1994. A revision of the garnet-clinopyroxene Fe^{2+}–Mg exchange geothermometer. *Contributions to Mineralogy and Petrology*, **115,** 467–473.

Berman, R. G., 1990. Mixing properties of Ca–Mg–Fe–Mn garnets. *American Mineralogist*, **75,** 328–344.

Canil, D. & O'Neill, H. St. C., 1996. Distribution of ferric iron in some upper-mantle assemblages. *Journal of Petrology*, **37,** 609–635.

Carswell, D. A. & Gibb, F. G. F., 1987. Garnet lherzolite xenoliths in the kimberlites of northern Lesotho: revised *P–T* equilibration conditions and upper mantle palaeogeotherm. *Contributions to Mineralogy and Petrology*, **97,** 473–487.

Carswell, D. A. & Zhang, R. Y., 1999. Petrographic characteristics and metamorphic evolution of ultrahigh-pressure eclogites in plate-collision belts. *International Geological Review*, **41,** 781–798.

Carswell, D. A., O'Brien, P. J., Wilson, R. J. & Zhai, M., 1997. Thermobarometry of phengite-bearing eclogites in the Dabie Mountains of central China. *Journal of Metamorphic Geology*, **15,** 239–252.

Carswell, D. A., Wilson, R. J. & Zhai, M., 2000. Metamorphic evolution, mineral chemistry and thermobarometry of schists and orthogneisses hosting ultra-high pressure eclogites in the Dabieshan of central China. *Lithos*, **52,** 121–155.

Chopin, C., 1984. Coesite and pure pyrope in high grade blueschists of the Western Alps: a first record and some consequences. *Contributions to Mineralogy and Petrology*, **86,** 107–118.

Coggon, R. & Holland, T. J. B., 2002. Mixing properties of phengitic micas and revised garnet-phengite thermobarometers. *Journal of Metamorphic Geology*, **20,** 683–696.

Connolly, J. A. D., 1990. Multivariable phase diagrams: an algorithm based on generalized thermodynamics. *American Journal of Science*, **290,** 666–718.

Cuthbert, S. J., Carswell, D. A., Ravna, E. J. K. & Wain, A. L., 2000. Eclogites and eclogites in the Western Gneiss Region, Norwegian Caledonides. *Lithos*, **52,** 165–195.

Dencker, I., Nimis, P., Zanetti, A. & Sobolev, N. V., 2003. Major and trace elements composition of Cr-diopsides from the Zagadochnaya kimberlite pipe (Yakutia, Russia): Insights into metasomatic processes in the Yakutian lithosphere. 8th International Kimberlite Conference Long Abstract.

Dobrzinetskaya, L. F., Schweinehage, R., Massone, H.-J. & Green, H. W., 2002. Silica precipitates in omphacite from eclogite at Alpe Arami, Switzerland: evidence of deep subduction. *Journal of Metamorphic Geology*, **20,** 481–492.

Ellis, D. J. & Green, D. H., 1979. An experimental study of the effect of Ca upon the garnet–clinopyroxene Fe–Mg exchange equilibria. *Contributions to Mineralogy and Petrology*, **71,** 13–22.

Ernst, W. G., 1977. Mineralogic study of eclogitic rocks from Alpe Arami, Lepontine Alps, southern Switzerland. *Journal of Petrology*, **18,** 371–398.

Ganguly, J., Cheng, W. & Tirone, M., 1996. Thermodynamics of aluminosilicate garnet solid solution: new experimental data, an optimized model, and thermometry applications. *Contributions to Mineralogy and Petrology*, **126,** 137–151.

Gilotti, J. A. & Ravna, E. J. K., 2002. First evidence for ultra-high-pressure metamorphism in the North-East-Greenland Caledonides. *Geology*, **30,** 551–554.

Heinrich, C. A., 1986. Eclogite facies regional metamorphism of hydrous mafic rocks in the central alpine Adula nappe. *Journal of Petrology*, **27,** 123–154.

Holland, T. J. B., 1990. Activities of components in omphacite solid solutions. *Contributions to Mineralogy and Petrology*, **105,** 446–453.

Holland, T. J. B. & Powell, R., 1990. An enlarged and updated internally consistent thermodynamic dataset with uncertainties and correlations: The system K_2O–Na_2O–CaO–MgO–MnO–FeO–Fe_2O_3–Al_2O_3–TiO_2–SiO_2–C–H_2–O_2. *Journal of Metamorphic Geology*, **8,** 89–124.

Holland, T. J. B. & Powell, R., 1998. An internally-consistent thermodynamic dataset for phases of petrological interest. *Journal of Metamorphic Geology*, **16,** 309–343.

Krabbendam, M. & Wain, A. L., 1997. Late Caledonian structures, differential retrogression and structural position of (ultra)high-pressure rocks in the Nordfjord-Stadlandet area, Western Gneiss Region. *Norges* Geologiske Undersøkelse Bulletin, **432,** 127–139.

Krogh, E. J., 1980. Geochemistry and petrology of glaucophane-bearing eclogites and associated rocks from Sunnfjord, Western Norway. *Lithos*, **13,** 355–380.

Krogh, E. J., 1988. The garnet–clinopyroxene Fe–Mg geothermometer: a reinterpretation of existing experimental data. *Contributions to Mineralogy and Petrology*, **99,** 44–48.

Krogh, E. J., Oh, C. W. & Liou, J. G., 1994. Polyphase and anticlockwise *P–T* evolution for Franciscan eclogites and blueschists from Jenner, California, USA. *Journal of Metamorphic Geology*, **12,** 121–134.

Liou, J. G., Zhang, R.-Y., Katayama, I, Maruyama, S. & Ernst, W. G., 2002. Petrotectonic characterization of the Kokchetav massif and the Dabie-Sulu terrane – ultrahigh-P metamorphism in the so-called *P–T* forbidden zone. *Western Pacific Earth Sciences*, **2,** 119–148.

Meyre, C., de Capitani, C., Zack, T. & Frey, M., 1999. Petrology of high-pressure metapelite from the Adula Nappe (Central Alps, Switzerland). *Journal of Petrology*, **40,** 199–213.

Nakamura, D. & Banno, S., 1997. Thermodynamic modeling of sodic pyroxene solid solution and its application in a garnet–omphacite–kyanite–coesite geothermobarometer for UHP metamorphic rocks. *Contributions to Mineralogy and Petrology*, **130,** 93–102.

Newton, R. C. & Haselton, H. T., 1981. Thermodynamics of the plagioclase–Al_2SiO_5–quartz geobarometer. In: *Thermodynamics of Minerals and Melts* (eds Newton, R. C., Navrotsky, A. & Wood, B. J.), pp. 131–148. Springer-Verlag, New York.

Nimis, P. & Taylor, W. R., 2000. Single clinopyroxene thermobarometry for garnet peridotites. Part I. Calibration and testing of a Cr-in-Cpx barometer and an enstatite-in-Cpx thermometer. *Contributions to Mineralogy and Petrology*, **139,** 541–554.

Nimis, P. & Trommsdorff, V. 2001a. Revised thermobarometry of Alpe Arami and other garnet peridotites from the central Alps. *Journal of Petrology*, **42,** 103–115.

Nimis, P. & Trommsdorff, V. 2001b. Comments on 'New constraints on the *P–T* evolution of the Alpe Arami garnet peridotite body (Central Alps, Switzerland)' by Paquin & Altherr (2001). *Journal of Petrology*, **42,** 1773–1779.

Nowlan, E. U., Schertl, H.-P. & Schreyer, W., 2000. Garnet–omphacite–phengite thermobarometry of eclogites from the coesite-bearing unit of the southern Dora-Maira Massif, Western Alps. *Lithos*, **52,** 197–2000.

Okamoto, K. & Maruyama, S., 1999. The high-pressure synthesis of lawsonite in the MORB + H_2O system. *American Mineralogist*, **84,** 362–373.

Okay, A. I., 1983. Petrology of a diamond- and coesite-bearing metamorphic terrain: Dabie Shan, China. *European Journal of Mineralogy*, **5,** 659–675.

Paquin, J. & Altherr, R., 2001a. New constraints on the *P–T* evolution of the Alpe Arami garnet peridotite body (Central Alps, Switzerland). *Journal of Petrology*, **42,** 1119–1140.

Paquin, J. & Altherr, R., 2001b. 'New constraints on the *P–T* evolution of the Alpe Arami garnet peridotite body (Central Alps, Switzerland)': Reply to Comment by Nimis & Trommsdorff (2001). *Journal of Petrology*, **42,** 1781–1787.

Pattison, D. R. M. & Newton, R. C., 1989. Reversed experimental calibration of the garnet–clinopyroxene Fe–Mg exchange thermometer. *Contributions to Mineralogy and Petrology*, **101,** 87–103.

Powell, R., 1985. Regression diagnostics and robust regression in geothermometer/geobarometer calibration: the garnet–clinopyroxene geothermometer revisited. *Journal of Metamorphic Geology*, **3,** 231–243.

Powell, R. & Holland, T. J. B., 1988. An internally consistent thermodynamic dataset with uncertainties and correlations: 3. Applications to geobarometry, worked examples and a computer program. *Journal of Metamorphic Geology*, **6,** 173–204.

Ravna, E. J. K., 2000. The garnet–clinopyroxene geothermometer – an updated calibration. *Journal of Metamorphic Geology*, **18,** 211–219.

Ravna, E. J. K. & Paquin, J., 2004. Thermobarometric methodologies applicable to eclogites and garnet ultrabasites. *EMU Notes in Mineralogy*, vol. **5,** Ch. 8, 229–259.

Ravna, E. J. K. & Terry, M. P., 2001. Geothermobarometry of phengite–kyanite–quartz/coesite eclogites. Eleventh Annual V. M. Goldschmidt Conference, abstract 3145.

Schmid, R., (2001). Geology of Ultra-High-Pressure Rocks from the Dabie Shan, Eastern China. *Dissertation am Institut für Geowissenschaften der Universität Potsdam*, 141 pp.

Schmid, R., Wilke, M., Oberhänsli, R. *et al.*, 2003. Micro-XANES determination of ferric iron and its application in thermobarometry. *Lithos*, **70,** 381–392.

Schulze, D. J., Helmstaedt, H., 1988. Coesite–sanidine eclogites from kimberlite: products of mantle fractionation or subduction. *Journal of Geology*, **96,** 435–443.

Schulze, D. J., Valley, J. M. & Spicuzza, M. J., 2000. Coesite eclogites from the Roberts Victor kimberlite, South Africa. *Lithos*, **54,** 23–32.

Sharp, Z. D., Essene, E. J. & Smyth, J. R., 1992. Ultra-high temperatures and pressures from oxygen isotope thermometry of a coesite–sanidine grospydite. *Contributions to Mineralogy and Petrology*, **112,** 358–370.

Smith, D. C., 1984. Coesite in clinopyroxene in the Caledonides and its implications for geodynamics. *Nature*, **310,** 641–644.

Sobolev, V. N., McCammon, C. A., Taylor, L. A., Snyder, G. A. & Sobolev, N. V., 1999. Precise Mössbauer milliprobe determination of ferric iron in rock-forming minerals and limitations of electron microprobe analyses. *American Mineralogist*, **84,** 78–85.

Terry, M. P., Robinson, P. & Ravna, E. J. K., 2000. Kyanite eclogite thermobarometry and evidence for thrusting of UHP over HP metamorphic rocks, Nordøyane, Western Gneiss Region, Norway. *American Mineralogist*, **85,** 1637–1650.

Wain, A., 1998. *Ultrahigh-pressure metamorphism in the Western Gneiss region of Norway*. D. Phil. Thesis, University of Oxford, Oxford.

Wain, A., Waters, D. J. & Austrheim, H., 2001. Metastability of granulites and processes of eclogitisation in the UHP region of western Norway. *Journal of Metamorphic Geology*, **19,** 609–625.

Waters, D. J. & Martin, H. N., 1993. Geobarometry of phengite-bearing eclogites. *Terra Abstracts*, **5,** 410–411.

Waters, D. J. & Martin, H. N., 1996. The Garnet-Cpx-Phengite Barometer. Recommended calibration and calculation method, updated 1 March 1996. http://www.earth.ox.ac.uk/~davewa/research/eclogites/ecbarcal.html.

Zack, T., Rivers, T. & Foley, S. F., 2001. Cs–Rb–Ba systematics in phengite and amphibole: an assessment of fluid mobility at 2.0 Gpa in eclogites from Trescolmen, Central Alps. *Contributions to Mineralogy and Petrology*, **140,** 651–669.

Zack, T., Foley, S. F. & Rivers, T., 2002. Equilibrium and disequilibrium trace element partitioning in hydrous eclogites (Trescolmen, Central Alps). *Journal of Petrology*, **43,** 1947–1974.

Received 8 October 2002; revision accepted 22 May 2004.

APPENDIX 1

Activity models for grossular and pyrope, respectively (Ganguly *et al.*, 1996).

$$\begin{aligned} RT\ln\gamma_{\mathrm{Ca}} = {} & (1-2X_{\mathrm{Ca}})(W_{\mathrm{CaMg}}X_{\mathrm{Mg}}^2 + W_{\mathrm{CaFe}}X_{\mathrm{Fe}}^2) + 2(1-X_{\mathrm{Ca}})(W_{\mathrm{MgCa}}X_{\mathrm{Mg}}X_{\mathrm{Ca}} + W_{\mathrm{FeCa}}X_{\mathrm{Ca}}X_{\mathrm{Fe}}) \\ & - 2(W_{\mathrm{MgFe}}X_{\mathrm{Mg}}X_{\mathrm{Fe}}^2 + W_{\mathrm{FeMg}}X_{\mathrm{Fe}}X_{\mathrm{Mg}}^2 + W_{\mathrm{MgMn}}X_{\mathrm{Mg}}X_{\mathrm{Mn}}^2 + W_{\mathrm{MnMg}}X_{\mathrm{Mn}}X_{\mathrm{Mg}}^2 + W_{\mathrm{MnFe}}X_{\mathrm{Mn}}X_{\mathrm{Fe}}^2 \\ & + W_{\mathrm{FeMn}}X_{\mathrm{Fe}}X_{\mathrm{Mn}}^2) + 0.5(1-2X_{\mathrm{Ca}})(X_{\mathrm{Mg}}X_{\mathrm{Fe}}(W_{\mathrm{CaMg}} + W_{\mathrm{MgCa}} + W_{\mathrm{CaFe}} + W_{\mathrm{FeCa}} + W_{\mathrm{MgFe}} + W_{\mathrm{FeMg}}) \\ & + X_{\mathrm{Mg}}X_{\mathrm{Mn}}(W_{\mathrm{CaMg}} + W_{\mathrm{MgCa}} + W_{\mathrm{MgMn}} + W_{\mathrm{MnMg}}) + X_{\mathrm{Fe}}X_{\mathrm{Mn}}(W_{\mathrm{CaFe}} + W_{\mathrm{FeCa}} + W_{\mathrm{FeMn}} + W_{\mathrm{MnFe}})) \\ & - X_{\mathrm{Mg}}X_{\mathrm{Fe}}X_{\mathrm{Mn}}(W_{\mathrm{MgFe}} + W_{\mathrm{FeMg}} + W_{\mathrm{MgMn}} + W_{\mathrm{MnMg}} + W_{\mathrm{FeMn}} + W_{\mathrm{MnFe}}) \end{aligned}$$

$$\begin{aligned} RT\ln\gamma_{\mathrm{Mg}} = {} & (1-2X_{\mathrm{Mg}})(W_{\mathrm{MgCa}}X_{\mathrm{Ca}}^2 + W_{\mathrm{MgFe}}X_{\mathrm{Fe}}^2 + W_{\mathrm{MgMn}}X_{\mathrm{Mn}}^2) + 2(1-X_{\mathrm{Mg}})(W_{\mathrm{CaMg}}X_{\mathrm{Mg}}X_{\mathrm{Ca}} \\ & + W_{\mathrm{FeMg}}X_{\mathrm{Mg}}X_{\mathrm{Fe}} + W_{\mathrm{MnMg}}X_{\mathrm{Mn}}X_{\mathrm{Mg}}) - 2(W_{\mathrm{CaFe}}X_{\mathrm{Ca}}X_{\mathrm{Fe}}^2 + W_{\mathrm{FeCa}}X_{\mathrm{Fe}}X_{\mathrm{Ca}}^2 + W_{\mathrm{MnFe}}X_{\mathrm{Mn}}X_{\mathrm{Fe}}^2 \\ & + W_{\mathrm{FeMn}}X_{\mathrm{Fe}}X_{\mathrm{Mn}}^2) + 0.5(1-2X_{\mathrm{Mg}})(X_{\mathrm{Ca}}X_{\mathrm{Fe}}(W_{\mathrm{MgCa}} + W_{\mathrm{CaMg}} + W_{\mathrm{MgFe}} + W_{\mathrm{FeMg}} + W_{\mathrm{CaFe}} + W_{\mathrm{FeCa}}) \\ & + X_{\mathrm{Ca}}X_{\mathrm{Mn}}(W_{\mathrm{MgCa}} + W_{\mathrm{CaMg}} + W_{\mathrm{MgMn}} + W_{\mathrm{MnMg}}) + X_{\mathrm{Fe}}X_{\mathrm{Mn}}(W_{\mathrm{MgFe}} + W_{\mathrm{FeMg}} + W_{\mathrm{MgMn}} + W_{\mathrm{MnMg}} \\ & + W_{\mathrm{FeMn}} + W_{\mathrm{MnFe}})) - X_{\mathrm{Ca}}X_{\mathrm{Fe}}X_{\mathrm{Mn}}(W_{\mathrm{CaFe}} + W_{\mathrm{FeCa}} + W_{\mathrm{FeMn}} + W_{\mathrm{MnFe}}) \end{aligned}$$

$$W_{ij}^{G}(P,T) = W_{ij}^{H}(0.0001,T) - TW_{ij}^{S}(0.0001,T) + 10^4(P-1)W_{ij}^{V}$$

Internally consistent binary subregular interaction parameters in aluminosilicate garnets (Ganguly *et al.*, 1996).

Parameter (*ij*)	W_{ij}^{H}	W_{ij}^{S}	W_{ij}^{V}
CaMg	21 627	5.78	0.012
MgCa	9 834	5.78	0.058
CaFe	873	1.69	0
FeCa	6 773	1.69	0.03
MgFe	2 117	0	0.07
FeMg	695	0	0
MgMn	12 083	7.67	0.04
MnMg	12 083	7.67	0.03
FeMn	539	0	0.04
MnFe	539	0	0.01

Activity models for white mica (Holland & Powell, 1998)

$$a_{\mathrm{mu}}^{\mathrm{ideal}} = 4X_K^A X_{\mathrm{Al}}^{M2A} X_{\mathrm{Al}}^{T1} X_{\mathrm{Si}}^{T1}$$

$$a_{\mathrm{cel}} = X_K^{mu} X_{\mathrm{Mg}}^{M2A} (X_{\mathrm{Si}}^{T1})^2.$$

In this approximately ideal mixing model, it is suggested that Al and Mg (+ Fe^{2+}) can only mix on one (M2A) of the two octahedral sites. Here, the M1A site is first filled up with Al. The remaining Al and other cations (Ti, Cr, Mn) are located in the M2A site.

Activity models for diopside (Holland, 1990)

$$RT\ln\gamma_{\mathrm{CaMg}} = X_{\mathrm{Na}}^{M2}[X_{\mathrm{Fe3+}}^{M1}(W_{\mathrm{A}} - W_{\mathrm{C}}) + X_{\mathrm{Fe^{2+}}}^{M1}(W_{\mathrm{A}} - W_{\mathrm{B}}) + X_{\mathrm{Al}}^{M1}W_{\mathrm{A}}]$$

$$W_{\mathrm{A}} = 26\ \mathrm{kJ};\quad W_{\mathrm{B}} = 25\ \mathrm{kJ};\quad W_{\mathrm{C}} \approx 0.$$